J Nanostruct 9(2): 316-325, Spring 2019

RESEARCH PAPER

Synthesis and Nucleation Mechanism Recognition of $BaSO_4$ Nanoparticle in the Presence of Biopolymers

Mehrdad Manteghian *, Abdolhamid Sameni

Chemical Engineering Faculty, Tarbiat Modares University, Tehran, Iran

ARTICLE INFO

Article History:
Received 05 October 2018
Accepted 12 January 2019
Published 01 April 2019

Keywords:
$Baso_4$
Biopolymers
Induction Time
Nanoparticles

ABSTRACT

A major portion of $BaSO_4$ is used as drilling fluid additives in the presence of some biopolymers such as starch and PAC (Polyanionic Cellulose) as filtration control and viscosifier. $BaSO_4$ nanoparticle was synthesized in the presence of these applicable polymers with precipitation method by using BaS produced from carbothermal method and Na_2SO_4. Synthesized nanoparticles size and morphology were analyzed using DLS (Dynamic Light Scattering) and FESEM (Field Emission Scanning Electron Microscope). It can be concluded that, nanoparticles size have inverse proportion with polymer concentration. Also nanoparticles have smaller size in the presence of PAC with longer functional group than starch and prevent chemical reaction due to steric hindrance. If pH increases from 7 to 11, nanoparticles in starch had minimum size in pH=9 and various pH didn't have noticeable effect on size with PAC. In kinetic study, conductometer is used to detect induction time in different Na_2SO_4 concentrations and polymers and it is indicated that interfacial tension is decreased as reactant concentration increased and PAC increase induction time and reduce interfacial tension more than starch.

How to cite this article
Manteghian M, Sameni A. Synthesis and Nucleation Mechanism Recognition of $BaSO_4$ Nanoparticle in the Presence of Biopolymers. J Nanostruct, 2019; 9(2): 316-325. DOI: 10.22052/JNS.2019.02.013

INTRODUCTION

Over 80% of the total $BaSO_4$ (Barite) ore produced worldwide, is used in drilling fluids as a weighting additives and rest is applicable as filling material in plastic and paint industries [1]. Also $BaSO_4$ used in automobile industry as friction reduction and in ceramic and medical application. Some of special features of $BaSO_4$ are its low solubility, chemical inertness and specific gravity of about 4-4.5. It is also non-abrasive, soft and easily ground, inexpensive and accessible now [2].

Top Down process such as ball milling and Bottom Up process such as precipitation of BaS generated from carbothermal of barite with Na_2SO_4 are the customary methods of producing $BaSO_4$ in industrial scale. Carbothermal reduction is a reaction using carbon as the reducing agent at high temperature. Recently, the applications of nanosize barite such as resin and rubber were studied [3].

Petrova used $BaCl_2$ and KSO_4 as reactants in stirrer tank reactor to synthesize barite nanoparticle and concluded that mechanical mixing and molar ratio of the reactants have effect on size [4]. Ramaswamy worked with $BaCl_2$ and NH_4SO_4 to produce $BaSO_4$ nanoparticles in water/ethanol and water/benzene as solvent [5, 6]. Bhari produced mesoporous $BaSO_4$ particles with high surface area via the reaction between $Ba(OH)_2$and H_2SO_4 with ethylene glycol as a modifying agent [7] and in another article with polycarboxylic polymer [8]. Jeremy precipitated barium sulfate as nanoparticle and nanofilaments [9]. Judat and Kind modeled $BaSO_4$ growth mechanism [10].

* *Corresponding Author Email: manteghi@modares.ac.ir*

Molaei synthesized barium sulfate with spinning disk reactor and studied some parameters which consist of disk rotation speed and diameter, supersaturation and free ion ratio [11]. Li modified barite nanoparticle with stearate and studied this modification effect on contact angle, surface energy, sedimentation rate and rheological properties [12]. Despite previous studies, L.Du used BaS with agitation of micro bubbles generated from continuous feed of N_2 gas in BaS and Na_2SO_4 feeds interaction to produce $BaSO_4$ nanoparticles in large scale application [3].

Some parameters are usually considered in the synthesis of nanoparticles such as induction time and mechanism of nucleation. In the crystallization process, induction time introduced the time between the addition of one reactant to another and first appearance of detectable change of solution. This phenomenon occurrence is nucleation and classified in primary and secondary categories. In order to find the mechanism of nucleation, the supersaturation and induction time should be measured. Induction time depends on S (Supersaturation), T (Temperature) and γ (Interfacial tension) and presence of impurities [4, 6] and seeds [5, 7] as external factors. Despite secondary nucleation, primary nucleation occurs without the presence of other crystallines.

Based on second principle of thermodynamics in crystallization theory, the required energy to create clusters of solute is related to surface and volume Gibbs free energy:

$$\Delta G = 4\pi r^2 \gamma + \left(\frac{4\pi}{3}\right) r^3 \Delta G_v \quad (1)$$

In Eq.1,γ is interfacial tension between surface of cluster and bulk of supersaturation solute and ΔGv is the required free energy for phase change. Derivation of Eq.1 to reach maximum value of G by considering the Gibbs-Thomson relation and inversely proportional assumption of nucleation rate and induction time, can lead to Eq.2:

$$t = k.\exp\left(\frac{-16\,\pi\,\gamma^3\,v^2}{3K^3T^3(\ln S)^2}\right) \quad (2)$$

Where *K* is the Boltzmann constant, *S* is supersaturation, v is molecular volume and *T* is temperature. Interfacial tension can be calculated from straight line slope (A) of plotted $\ln t_{ind}$ versus $\frac{1}{T^3(\ln S)^2}$ which can be achieved by taking the natural logarithm of both sides of Eq.2.[13]

$$A = \frac{16\,\pi\,\gamma^3\,v_m^2}{3K^3} \quad (3)$$

The mechanism of nucleation is determined with R^2 comparison of fitted line on data in mentioned plot and $\ln t_{ind}$ versus lnS plot which refer to secondary nucleation as Eq. 4

$$J = KS^b \quad (4)$$

Stabilizers reduce interfacial tension and prevent nuclei from growing. Therefore, their performance can be measured by finding the slope of primary nucleation graph and interfacial tension is calculated according to Eq.3.

Leeden investigated $BaSO_4$ deposits in the presence and lack of copolymers in seeded and unseeded precipitation [14]. Akyol studied the influence of polyelectrolytes concentration as size controller, pH of solution, the ratio of Ba and temperature on size and morphology of barium sulfate crystals [15]. Dera studied prevention from $BaSO_4$ deposits in pipes which can hinder the flow rate and lower heat transfer efficiency in various Ba^+ concentration, temperature and pH without presence of stabilizer [16]. Guo measured induction time in the presence of ultrasonic waves and concluded that induction time decreases by increasing energy input [17]. Matynia calculated the kinetics of barite crystallization with ammonium sulfate [18]. Manteghian measured induction time of various nanoparticles such as silver, potassium chloride in precipitation and antisolvent methods [19, 20]. In all of these papers, barite was crystallized with highly reactive chemicals as size controller with biological risks and poses potential environmental risk. To minimize and eliminate waste and promote sustainable processes as government's environmental regulations, the development of new green chemistry approaches is desirable [21]. These methodologies studied at Hassanpour paper which Methylene blue and Rhodamine B dyes in wastewater of industries removed with green synthesized Co_3O4/ZnO nanocomposite [22]. Also green synthesis of nanostructures was noticed in Zinatloo's study by using juice of ponica granatum as fuel and metal nitrate [23]. Green polymers are most applicable in oil and gas drilling fluid such as biocompatible additives like starch and PAC (Polyanionic Cellulose).

Starches $(C_6H_{10}O_5)_n$ are inexpensive and available biopolymers extracted from corn, wheat, oats, rice, potatoes, maize, yucca etc. Amylose (Linear polymer) and amylopectin (branched polymer) are the main parts of starches which are intertwined within starch granules and their percentage can be fractionated using a size exclusion column chromatography (SEC). Granules are insoluble in cold water but dispersed in warm water [24-26]. The uses of starches due to their environmentally friendly nature have recently become important for the synthesis of nanomaterial as size controller, especially in food and medical application [21, 27, 28].

PAC is a kind of nonionic cellulose ether with higher degree of carboxymethyl and the properties of high viscosity or low viscosity. These products are semi-natural polymer additive, thickening agent, filtrate reducer and used in drilling fluid as filtration reducer agent [29].

This study focuses on $BaSO_4$ kinetic crystallization and nucleation mechanism and also synthesis of barite nanoparticle by starch and PAC biopolymers in different pH which have real application in oil and gas drilling fluid.

MATERIALS AND METHODS

In order to synthesize $BaSO_4$ nanoparticle, BaS was provided from carbothermal reduction of barite at 1100 °C. The produced BaS is soluble in water and was separated from unreacted carbon and barite with centrifuge. Barite was prepared from Dae June Co. and Merck while activated carbon was used as reducing agent. Na_2SO_4 was prepared from Dae June Co. to precipitate $BaSO_4$ nanoparticle. In this study, industrial form starch and PAC (Polyanionic Cellulose) were provided from drilling field as stabilizers.

Nanoparticle Synthesis

$BaSO_4$ nanoparticles were produced with starch and PAC as biopolymer size controller and the effect of their concentration and pH on nanoparticles size was studied.

In this study, 6 g of Na_2SO_4 was dissolved in 200 cc water in order to reduce unavoidable experimental errors. Then 3 g of starch and PAC was dissolved in two separate 200 cc beakers and was placed in a heat stirrer and the temperature was raised to 80 °C during mixing to separate impurities of industrial stabilizer and amylopectin fraction of starch [24]. Then it was centrifuged at 4000 rpm and they were removed from the solution.

First, 20 cc of stabilizer solution was poured in 50 cc beaker and mixed with 4.5 cc Na_2SO_4 solution on stirrer. The pH of prepared solution can increase at base range with $Ca(OH)_2$ as drilling fluid with the desire pH range (7-11) and mix for 10 min. Then stabilizers concentration effects were studied. Produced BaS concentration which was provided from carbothermal reaction, was measured with gravimetric method. The concentration of BaS was 0.631 M. A 2 cc of BaS solution was diluted to 5 cc and 0.5 cc of it was added dropwise in a container in 5 min. Produced $BaSO_4$ nanoparticles have white color and size distribution was measured with DLS (Dynamic Light Scattering) and image was taken with FESEM (Field Emission Scanning Electron Microscope) to study the size and morphology of nanoparticles and stabilizers coating status.

Induction Time

In this part, crystallization kinetics of $BaSO_4$ was studied. In some articles, bulk methods were used to detect induction time of crystals visually [19, 20], but in $BaSO_4$ crystallization due to low solubility product (k_{sp}), supersaturation of reactant in precipitation method should be too low and induction time can't be detectable and measurable. This diluted reactant and white color of $BaSO_4$ nanoparticles make the nucleation invisible. In order to solve this problem, conductometer was used to record induction time in such a way that by first adding reactant to water, quantity of ions increased, and conductivity also increased, when second reactant was added to the solution, reaction took place and amount of ions will reduce and conductivity will decrease.

Na_2SO_4 and different stabilizers in various concentrations were stirred in 100 cc distilled water and conductometer probe was put in a beaker and the conductivity was measured in micro siemens scale. Thereafter, solution was stirred and reached stable conductivity, BaS solution was added dropwise to beaker in various concentrations. Thereafter, each drop was added to the system, conductivity was recorded for 5 min. As shown in Fig.1, before the occurrence of nucleation, each drop increased the conductivity due to addition of ions to the system, and then conductivity trend is descending.

Induction time in this study was recorded at two series. First, effect of Na_2SO_4 concentration includes 5, 10, 20 and 30 mg/100 cc on nucleation and interfacial tension was studied. Then PAC and

starch performance at constant 1000 mg/100 cc concentration and 20 mg/100 cc of Na_2SO_4 was evaluated. In this study, supersaturation was introduced as initial concentration of BaS (at the moment of adding the last drops of BaS), divided by the equilibrium concentration of barium ion in the solution (C*) which is measured with atomic adsorption.

When the experiments were done, the samples were kept for 24 h, then a sample was obtained from the top of the fluid in a beaker, and equilibrium concentration of barium was measured with AAS. This data was repeated to check the results and their mean value was calculated.

RESULTS AND DISCUSSION

Nanoparticle Synthesis

Results of pH and stabilizers concentration on $BaSO_4$ nanoparticles particle size distribution which were analyzed with DLS and presented in Table 1 showed that biopolymers play the role of size controller in $BaSO_4$ nanoparticles synthesis via the network structure, through polymeric chains which consist of carboxyl and hydroxyl groups. Mean size of nanoparticle decreased as concentration of starch and PAC increased. If the performance of PAC and starch is compared in Fig.2a, 2b, it can be concluded that synthesized nanoparticle with PAC has smaller particle than

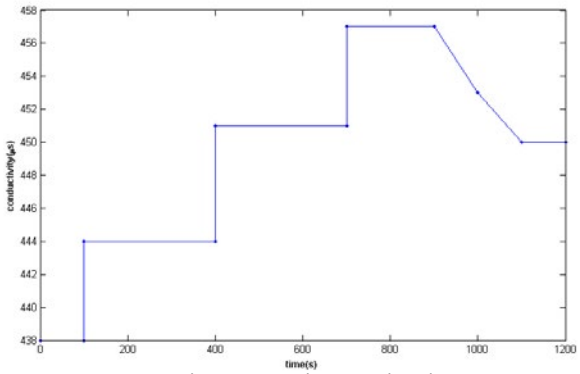

Fig. 1. Conductivity trend in crystal nucleation

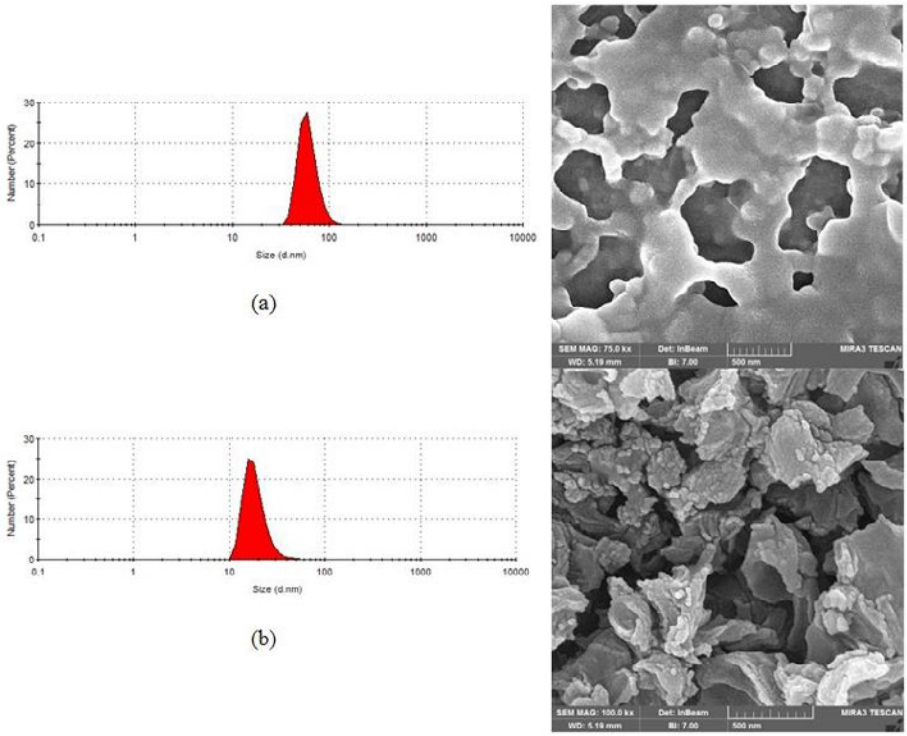

Fig. 2. DLS and FESEM analysis of $BaSO_4$ nanoparticles in presence of polymers at pH=7, (a) Starch, (b) PAC

starch. In description of this result, as shown in Fig.3, PAC has longer functional group than starch and prevents chemical reaction due to steric hindrance. This phenomenon can be seen in filtration volume of drilling fluid in the presence of these two polymers that volume of filtration for fluid with PAC is less than in same condition of starch and fluid with PAC has higher viscosity than starch. In FESEM images of samples analyzed with DLS, coating of nanoparticle with polymers is visible and their morphologies are spherical in shape.

Other results can be derived from Table 1, in the presence of starch as pH increased, size of nanoparticles decreased and then increased, but pH has no wide effect on PAC function. In explanation of these results, some studies stated that starch performance is enhanced if pH increases to 10 and then starch is degraded especially the amylose portion. This behavior of starch can be justified with mud engineer experience in drilling field [26, 30-32].

Synthesized nanoparticle XRD, EDX and FTIR are presented in Fig.4 .XRD analysis of the $BaSO_4$ nanoparticles (Fig. 4a) demonstrate that synthesized nano powder was pure and all of picks were according to 0020-024 reference patterns. FTIR spectroscopy is a useful technique to characterize inorganic compounds. Figure.4b shows FTIR spectrum of prepared $BaSO_4$ nanoparticles. The observed wave numbers are 3296, 1595, 1179, 1123, 1073, 982, 635 and 610 cm^{-1}. Alder showed that sulfur-oxygen (S-O) stretching of inorganic sulfates are found in the region 1200 - 1080cm^{-1}. The bands centered at 1179 to 1073 cm^{-1} and the shoulder at 982 cm^{-1} is the vibration of sulfate group [33]. According to Shen's study the peaks at 608 and 637cm^{-1} are due to the out-of-plane bending vibration of the SO_4^{2-}. The absorption peaks appeared at about 3433 and 1595cm^{-1} are due to the stretching and deformation of adsorbed water molecule [34]. Figure.4c shows the energy dispersive spectrum (EDS) of the $BaSO_4$ particles which clearly show the presence of Ba, S, and O elements.

As mentioned in introduction some papers have studied about $BaSO_4$ production which can be compared with this study at Table 2.

Induction Time

Collected supersaturation data and induction time were plotted according to nucleation theories. Various Na_2SO_4 concentration effects were studied in Fig.5, 6. From the comparison of R-Square of fitted data in Table 3, it was concluded that the mechanism of nucleation is primary nucleation. As shown, induction time decreased as the concentration of Na_2SO_4 increased.

In Eq.1, γ is interfacial tension (J/m^2), k = $1.3805*10^{-23}$ J/K, V_m= $8.613*10^{-29}$, which is

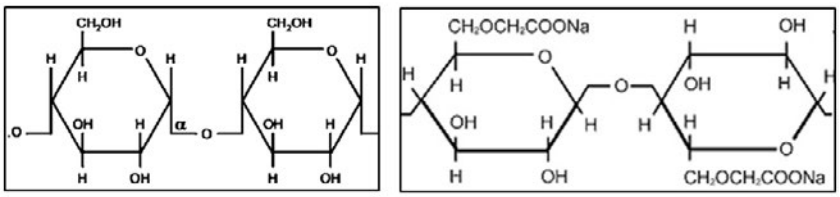

Fig. 3. Schematic of polymers structure, (a) starch, (b) PAC

Table 1. $BaSO_4$ nanoparticles size in different pH and polymers concentration

Stabilizers	Stabilizer Conc. (mg/25cc)	Na_2SO_4 Conc. (mg/25cc)	pH	BaS Conc. (mg/25cc)	Size (d.nm)	Mean Size
Starch	300	135	7	21.3	33-140	58.7
	300	135	9	21.3	21-91	38
	300	135	11	21.3	37-141	58.7
	400	135	9	21.3	6-32	9
	500	135	9	21.3	3-16	6
PAC	300	135	7	21.3	10-58	18
	300	135	9	21.3	9-37	14
	300	135	11	21.3	9-25	14
	400	135	9	21.3	4-18	8
	500	135	9	21.3	6-16	8

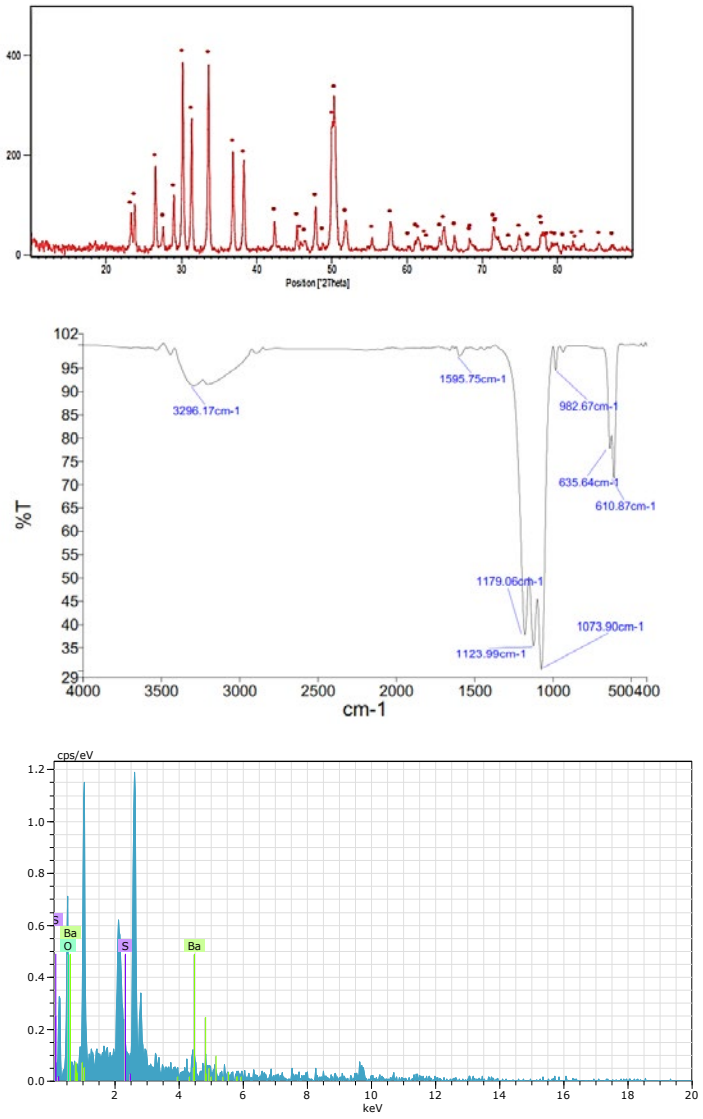

Fig. 4. Pure $BaSO_4$ synthesized nanoparticles characterization, (a) XRD, (b) FT-IR, (c) EDS

Table 2. Comparison of this study with other ones to synthesize BaSO4 nanoparticles

Reactant (Ba^+)	Reactant (SO_4^-)	Stabilizers	Investigated parameters	Results
$BaCl_2$	KSO_4	Polyether carboxylate	- Feed rate of KSO_4 - Molar ratio (Ba^+/ SO_4^-)	- As feed rate increased, particle size increased - As molar ratio increased, particle size decreased [4]
$BaCl_2$	Na_2SO_4	Water-benzene mixed solvent	- Different percentages of water-benzene	- Maximum particle size synthesized at 50 % water-benzene mixture with 50 nm [6]
BaS	Na_2SO_4	Microbubble method	- Reactant concentration and feed rate - Temperature	- As Na_2SO_4 feed rate increased, particle size decreased - As Na_2SO_4 concentration increased, particle size increased [3]
BaS	Na_2SO_4	Starch, PAC	- Polymers concentration - pH	- Particle size in presence of PAC smaller than starch - As polymer concentration increased, particle size decreased - As pH increased in starch first particle size decreased and then increased [This Study]

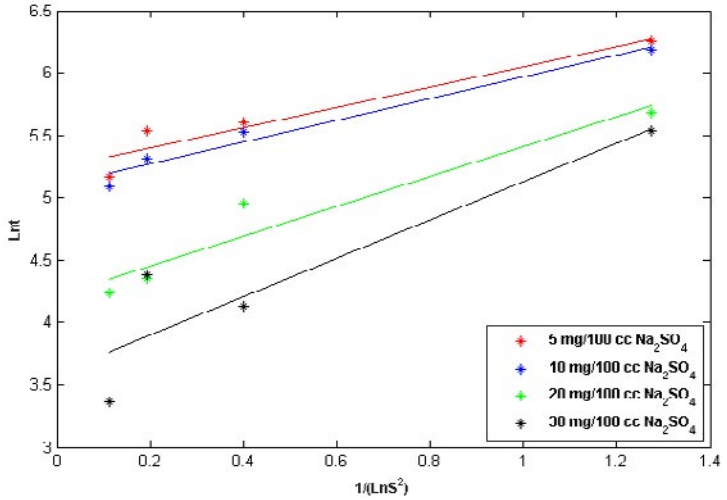

Fig. 5. $BaSO_4$ crystallization in different Na_2SO_4 concentrations based on primary nucleation theory

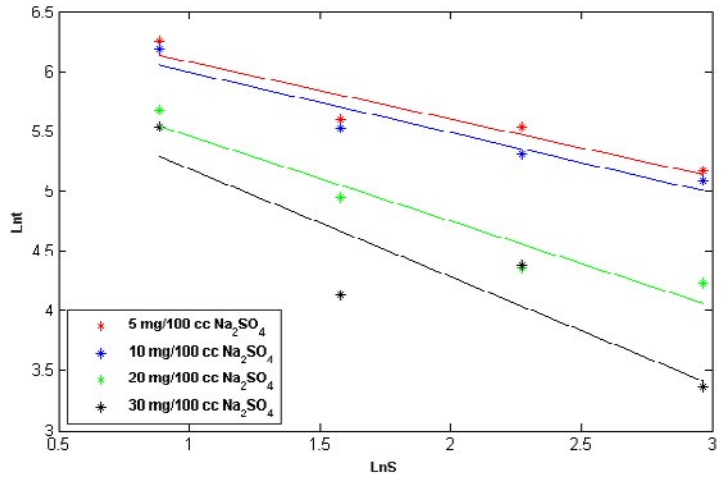

Fig. 6. $BaSO_4$ crystallization in different Na_2SO_4 concentrations based on secondary nucleation theory

Table 3. R-Square comparison between primary and secondary nucleation theories

Concentration	Primary R-Square	Secondary R-Square
5	0.91	0.90
10	0.97	0.91
20	0.93	0.92
30	0.83	0.80

calculated from $v_M = \frac{M_{BaSO4}}{\rho N_A}$ using M = 0.2334 kg/mol, q = 4500 kg/m^3 and N_{AA}= 6.023 · 10^{23} no. / mol.

$$\gamma = k\left(\frac{3A}{16\pi v_M^2}\right)^{\frac{1}{3}}$$

$$v_M = \frac{M_{BaSO4}}{\rho N_A} = \frac{0.2334}{4500 \times 6.022 \times 10^{23}} = 8.613 \times 10^{-29}$$

$$\gamma = 1.3805 \times 10^{-23}\left(\frac{3 \times 21{,}497{,}966.73}{16\pi(8.613 \times 10^{-29})^2}\right)^{\frac{1}{3}} = 7.69\ \frac{mj}{m^2}$$

The theoretically calculated values of interfacial tension are shown in Table 4. Based on this table, the interfacial tension is increased as concentration of Na_2SO_4 increased. When the concentration of Na_2SO_4 increased the chance of collision between reactant ions increased and interfacial tension is increased, therefore induction time is decreased according to Eq.2.

If the interfacial tension calculation is applied on different types of stabilizers as plotted in Fig.7,

Table 4. Interfacial tension various concentration of Na_2SO_4

C (Na_2SO_4) mg/100 cc	A	$\gamma(\frac{mj}{m^2})$
5	21,497,966.73	7.69
10	23,051,997.97	7.87
20	31,686,012.78	8.75
30	40,683,583.55	9.51

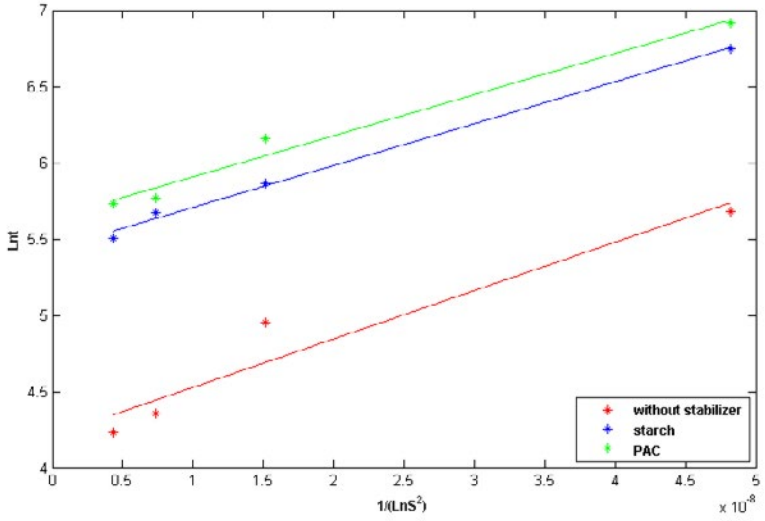

Fig. 7. $BaSO_4$ crystallization in different polymers on primary nucleation theory

Table 5. Interfacial tension in various concentration polymers

Polymers	A	$\gamma(\frac{mj}{m^2})$
Without Stabilizer	31,686,012.78	8.75
Starch	27,420,472.27	8.34
PAC	26,928,969.49	8.29

it can be presented in Table 5. PAC has higher level induction time and decreases the interfacial tension more than starch. Long chain of PAC can be described as the main reason for full coating of the cluster and reduced interfacial tension.

CONCLUSION

Starch and PAC are the polymers used in drilling fluid as filtration agent and barite is used as weighting material. In this paper, $BaSO_4$ nanoparticle was synthesized and nucleation was studied in the presence of these polymers. Analysis of synthesized nanoparticles showed that size of nanoparticles decrease as concentration of polymer increased. Nanoparticles are coated with polymers which are visible in FESEM and prevent the growth of particles. When the stabilizer was PAC, the size of nanoparticle was larger than starch. This phenomenon occurred because the PAC has longer functional group than starch and prevents chemical reaction due to steric hindrance. Furthermore, more effective function of PAC was confirmed with better filtration effect of PAC versus starch. Increase of pH at basement reduced the size of nanoparticle in starch stabilizer, but didn't have huge effect on PAC performance. It can be described that pH activates the starch chain despite PAC. Nucleation theories were applied on induction time to measure data of $BaSO_4$ with different stabilizer and reactant concentrations. Result of this study is in line with synthesis section result in such a way that PAC with longer chain increased induction time and decreased interfacial tension rather than starch by better coverage of

clusters. Also, Na_2SO_4 concentration was studied and it was concluded that collision probability between ions increased as Na_2SO_4 concentration increased, induction time decreased and interfacial tension increased.

CONFLICT OF INTEREST

The authors declare that there are no conflicts of interest regarding the publication of this manuscript.

REFERENCES

1. Scott, P., C. Phillips, and L. Robinson. Economic considerations and impacts for using low grade barite. in AADE fluids conference and exhibition, Houston. 2010.
2. Conn L, Bruton JR, Rafferty M, Matlock W. Unique Micronized Weight Material Delivers Ultrathin NAF To Optimize ERD Drilling. SPE Annual Technical Conference and Exhibition: Society of Petroleum Engineers; 2007.
3. Du L, Wang YJ, Lu YC, Luo GS. Process intensification of BaSO4 nanoparticle preparation with agitation of microbubbles. Powder Technology. 2013;247:60-8.
4. Petrova A, Hintz W, Tomas J. Investigation of the Precipitation of Barium Sulfate Nanoparticles. Chemical Engineering & Technology. 2008;31(4):604-8.
5. Ramaswamy, V., R. Vimalathithan, and V. Ponnusamy, Preparation of barium sulphate nanocrystals in ethanol—water mixed solvents. Journal of Ceramic Processing Research, 2011. 12(2): p. 173-175.
6. Ramaswamy V, M. Vimalathithan R, Ponnusamy V. Synthesis Of Monodispersed Barium Sulphate Nanoparticles Using Water-benzene Mixed Solvent. Advanced Materials Letters. 2012;3(1):29-33.
7. Nagaraja, B.M., et al., Novel Method for the Preparation of Mesoporous BaSO 4 Material with Thermal Stability by Spray Pyrolysis. Bulletin of the Korean Chemical Society, 2008. 29(5): p. 1007-1012.
8. Ismaiel, M. and I. Mostafa, Synthesis of BaSo 4 nanoparticles by precipitation method using polycarboxylate as a modifier. American Journal of Nanotechnology, 2011. 2: p. 106-111.
9. Hopwood JD, Mann S. Synthesis of Barium Sulfate Nanoparticles and Nanofilaments in Reverse Micelles and Microemulsions. Chemistry of Materials. 1997;9(8):1819-28.
10. Judat B, Kind M. Morphology and internal structure of barium sulfate—derivation of a new growth mechanism. Journal of Colloid and Interface Science. 2004;269(2):341-53.
11. Dehkordi AM, Vafaeimanesh A. Synthesis of Barium Sulfate Nanoparticles Using a Spinning Disk Reactor: Effects of Supersaturation, Disk Rotation Speed, Free Ion Ratio, and Disk Diameter. Industrial & Engineering Chemistry Research. 2009;48(16):7574-80.
12. Li L-l, Hang J-z, Shi L-y. Surface modification of barite nanoparticles using stearate. Journal of Shanghai University (English Edition). 2009;13(4):296-300.
13. Thanh NTK, Maclean N, Mahiddine S. Mechanisms of Nucleation and Growth of Nanoparticles in Solution. Chemical Reviews. 2014;114(15):7610-30.
14. van der Leeden MC, Kashchiev D, Van Rosmalen GM. Precipitation of barium sulfate: Induction time and the effect of an additive on nucleation and growth. Journal of Colloid and Interface Science. 1992;152(2):338-50.
15. Akyol E, Aras Ö, Öner M. Control of barium sulfate crystallization in the presence of additives. Desalination and Water Treatment. 2013;52(31-33):5965-73.
16. Dera NS, Fatra F, Ivanto G, Muryanto S, Bayuseno AP. Phase Analysis and Crystal Morphology of Barium Sulphate Precipitated from The Laminar Flowing Water. IOP Conference Series: Materials Science and Engineering. 2017;202:012029.
17. Guo Z, Jones AG, Li N. Interpretation of the ultrasonic effect on induction time during BaSO4 homogeneous nucleation by a cluster coagulation model. Journal of Colloid and Interface Science. 2006;297(1):190-8.
18. Matynia A, Piotrowski K, Koralewska J. Barium sulphate crystallization kinetics in the process of barium ions precipitation by means of crystalline ammonium sulphate addition. Chemical Engineering and Processing: Process Intensification. 2005;44(4):485-95.
19. Manteghian, M. and A. Faravar, Induction time of induced crystallization of potassium chloride nanoparticles. Journal of Chemical, 2014.
20. Ghader S, Manteghian M, Kokabi M, Mamoory RS. Induction Time of Reaction Crystallization of Silver Nanoparticles. Chemical Engineering & Technology. 2007;30(8):1129-33.
21. Ortega-Arroyo L, Martin-Martinez ES, Aguilar-Mendez MA, Cruz-Orea A, Hernandez-Pérez I, Glorieux C. Green synthesis method of silver nanoparticles using starch as capping agent applied the methodology of surface response. Starch - Stärke. 2013;65(9-10):814-21.
22. Hassanpour M, Safardoust-Hojaghan H, Salavati-Niasari M. Degradation of methylene blue and Rhodamine B as water pollutants via green synthesized Co3O4/ZnO nanocomposite. Journal of Molecular Liquids. 2017;229:293-9.
23. Zinatloo-Ajabshir S, Salehi Z, Salavati-Niasari M. Green synthesis of Dy2Ce2O7 ceramic nanostructures using juice of Punica granatum and their efficient application as photocatalytic degradation of organic contaminants under visible light. Ceramics International. 2018;44(4):3873-83.
24. Green MM, Blankenhorn G, Hart H. Which starch fraction is water-soluble, amylose or amylopectin? Journal of Chemical Education. 1975;52(11):729.
25. Suortti T, Gorenstein MV, Roger P. Determination of the molecular mass of amylose. Journal of Chromatography A. 1998;828(1-2):515-21.
26. Lee JH, Han J-A, Lim S-T. Effect of pH on aqueous structure of maize starches analyzed by HPSEC-MALLS-RI system. Food Hydrocolloids. 2009;23(7):1935-9.
27. Zamiri R, Zakaria A, Ahangar HA, Darroudi M, Zak AK, Drummen GPC. Aqueous starch as a stabilizer in zinc oxide nanoparticle synthesis via laser ablation. Journal of Alloys and Compounds. 2012;516:41-8.
28. Vasileva P, Alexandrova T, Karadjova I. Application of Starch-Stabilized Silver Nanoparticles as a Colorimetric Sensor for Mercury(II) in 0.005 mol/L Nitric Acid. Journal of Chemistry. 2017;2017:1-9.
29. Li M-C, Wu Q, Song K, De Hoop CF, Lee S, Qing Y, et al. Cellulose Nanocrystals and Polyanionic Cellulose as Additives in Bentonite Water-Based Drilling Fluids: Rheological Modeling and Filtration Mechanisms. Industrial & Engineering Chemistry Research. 2015;55(1):133-43.

30. Han, J.-A. and S.-T. Lim, Structural changes in corn starches during alkaline dissolution by vortexing. Carbohydrate Polymers, 2004. 55(2): p. 193-199.
31. Muhrbeck P. Influence of pH and ionic strength on the viscoelastic properties of starch gels — A comparison of potato and cassava starches. Carbohydrate Polymers. 1987;7(4):291-300.
32. Nutting GC. Effect of electrolytes on the viscosity of potato starch pastes. Journal of Colloid Science. 1952;7(2):128-39.
33. Adler, H.H. and P.F. Kerr, Variations in infrared spectra molecular symmetry and site symmetry of sulfate minerals. American Mineralogist, 1965. 50(1-2): p. 132-&.
34. Shen Y, Li C, Zhu X, Xie A, Qiu L, Zhu J. Study on the preparation and formation mechanism of barium sulphate nanoparticles modified by different organic acids. Journal of Chemical Sciences. 2007;119(4):319-24.